Research Progress of Photocatalytic Technology on Marine Anti-Fouling Coatings

Bi Qiao-ling[1,2], Jiang Shao-yu[1], Wu Chun-jie[1], Wang Cun-guo[1,*], He Ai-hua[1,*] and Li Qi[2,*]

[1]*State Key Laboratory of Advanced Optical Polymer and Manufacturing Technology; Key Laboratory of Rubber-plastics, Ministry of Education; Shandong Province Key Laboratory of Function Rubbers Materials and Engineering; Qingdao University of Science and Technology, Qingdao 266042, China*

[2]*Key Laboratory of Nanodevices and Applications & Collaborative Innovation Center of Suzhou Nano Science and Technology, Suzhou Institute of Nano-Tech and NanoBionics, Chinese Academy of Sciences (CAS), Suzhou 215123, China*

Abstract: With the continued expansion of the shipping industry, marine biofouling has emerged as a persistent challenge for vessels and offshore structures. Conventional antifouling coatings, while effective, often rely on toxic compounds that pose serious risks to marine ecosystems, highlighting the urgent need for environmentally benign alternatives. Among emerging solutions, photocatalytic antifouling coatings have attracted growing interest due to their eco-friendly nature. This review examines the mechanisms underlying marine biofouling, contrasts the environmental impacts of traditional and photocatalytic antifouling approaches, and elucidates the working principles of photocatalytic systems. Recent research showed that zinc oxide nanoparticles inhibited the growth rates of Spirulina, Dunaliella salina, and Muelleria filamentosa by 90.88%, 94.06%, and 92.49%, respectively, demonstrating their high potential for effective inhibition. A systematic overview of key photocatalysts, including titanium dioxide, cadmium sulfide, and carbon nitride, is provided, covering their performance attributes, modification strategies, and recent advances in application.

Keywords: Biofouling, Anti-fouling Coatings, Photocatalysis.

1. INTRODUCTION

In recent years, the global shipping industry has grown rapidly, with the number of seagoing vessels steadily rising. This expansion has been accompanied by a growing challenge: marine biofouling. Organisms such as bacteria, diatoms, barnacles, and shellfish attach themselves to the surfaces of ships, subsea pipelines, and aquaculture cages, creating a significant technical obstacle for the marine economy. Worldwide, more than 40% of commercial vessels experience hard fouling coverage greater than 10%, leading to economic losses of up to $150 billion and contributing an additional 110 million tons of carbon emissions, as illustrated in Figure **1** [1-3]. For instance: (1) Increased vessel weight and hull roughness heighten navigation resistance, leading to higher energy consumption; (2) Exacerbated environmental pollution causes significant increases in harmful compounds like CO_2, SO_4^{2-}, and NO_x emitted by ships and marine structures [4]; (3) Accelerates structural degradation by increasing corrosion rates of underwater metal structures, shortening their service life; (4) Facilitates the spread of invasive species through ballast water and hull fouling, threatening ecological security [5-7].

To address the challenges posed by marine biofouling, antifouling coating technologies have become widely implemented. Historically, organotin-based paints were effective, but their high toxicity and persistence in the environment caused severe ecological harm. As a result, they were explicitly prohibited under international agreements. The International Maritime Organization (IMO) reinforced this restriction through amendments to the AFS Code, which officially came into effect on January 1, 2023 [8]. These amendments not only banned the use of organotin compounds in ship antifouling coatings but also extended the prohibition to toxic coatings containing cyclobutane. Consequently, the development of environmentally sustainable antifouling technologies has emerged as a critical research priority [9-11]. Among the alternatives, bionic antifouling coatings offer benefits such as biocompatibility and multifunctionality but are limited by poor mechanical strength and vulnerability to micro/nanostructural damage, often resulting in fouling failure. Similarly, controlling the degradation rate of main-chain degradable self-polishing coatings remains difficult, and reduced concentrations of antifouling agents during the later release stages lead to diminished effectiveness. To improve durability, integration with photocatalytic systems or bionic designs is often necessary. Nanocomposite coatings also show promise, but challenges such as poor nanoparticle dispersion and the need for precision equipment to achieve uniform nanomaterial loading drive up industrial costs. Of these emerging strategies,

*Address Correspondence to this Author at State Key Laboratory of Advanced Optical Polymer and Manufacturing Technology; Key Laboratory of Rubber-plastics, Ministry of Education; Shandong Province Key Laboratory of Function Rubbers Materials and Engineering; Qingdao University of Science and Technology, Qingdao 266042, China;
E-mail: wangcg@qust.edu.cn; ahhe@qust.edu.cn; qli2013@sinano.ac.cn

Received on 15-10-2025 Accepted on 27-12-2025 Published on 03-01-2026

E-ISSN: 000-000/26

Figure 1: Fouling costs upon the attachment to ship hull (such as barnacles, diatoms, shellfish, etc.), which cause serious problems in shipping industry [1].

photocatalytic antifouling coatings have attracted particular attention as a promising green solution, offering both effectiveness and environmental compatibility [12]. By harnessing light energy to drive catalysts such as TiO_2 and ZnO to generate highly reactive oxygen species (ROS) [13], these coatings efficiently degrade and inhibit the adhesion of microorganisms and algal spores without introducing environmental toxins, demonstrating substantial application potential. However, pure photocatalytic nanopowders struggle to function stably and sustainably in real marine environments. Therefore, it is crucial to firmly and uniformly anchor the nanocatalyst to the coating matrix by leveraging the characteristics of functional polymers and nanocomposites, thereby achieving highly efficient and continuous photocatalytic reactions. This paper reviews the anti-fouling mechanisms of marine organisms and elucidates the working principles of photocatalytic systems. It presents typical examples of modifying functional polymers with key photocatalytic antifouling agents such as titanium dioxide, cadmium sulfide, and carbon nitride as key photocatalytic antifouling agents combined with functional polymers as carriers and synergistic components, as well as various nanocomposites as active enhancement units for modification. It also outlines future development trends for this technology, aiming to provide theoretical foundations and technical references for developing next-generation highly efficient, long-lasting, and environmentally friendly marine antifouling solutions.

2. FORMATION MECHANISM OF MARINE BIOFOULING

The formation of marine biofouling is a complex process [14], broadly divided into four stages, as illustrated in Figure **2**:

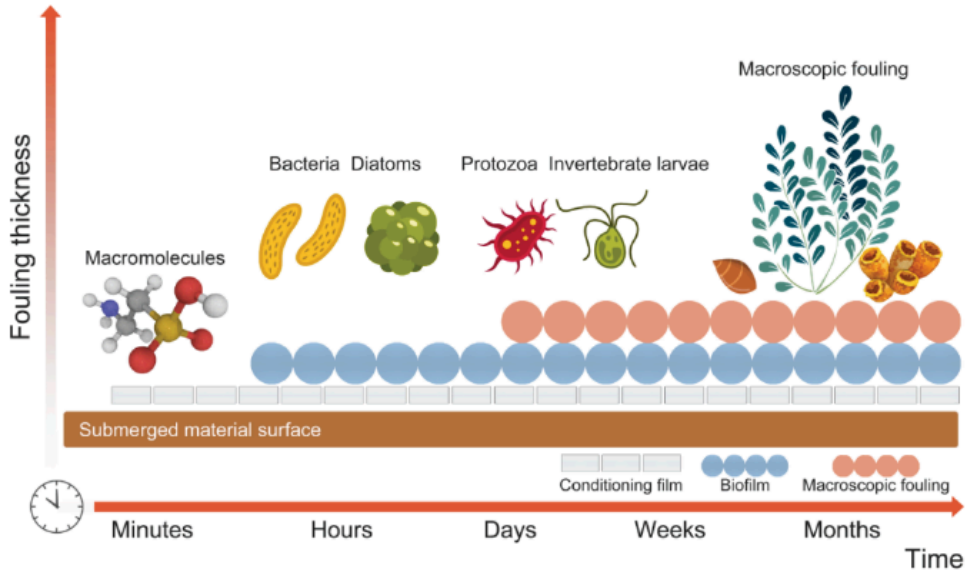

Figure 2: Schematic diagram of marine pollution formation process [14].

(1) Formation of the condition film: When marine structures are immersed in seawater, organic and inorganic substances rapidly adsorb onto their surfaces, forming a nanoscale film that alters the interfacial properties and creates conditions conducive to microbial attachment [15].

(2) Initial microbial adhesion stage: Bacteria, diatoms, and other organisms approach surfaces through physical interactions and transition from reversible attachment to irreversible fixation by secreting extracellular polymers (EPS) [16].

(3) Biofilm development stage: Microorganisms proliferate extensively, with EPS forming intricate three-dimensional structures, leading to increasingly diverse and stable microbial communities within the biofilm [17].

(4) Attachment stage of large fouling organisms: Mature biofilms provide critical signals and substrates for the attachment of large fouling organisms such as barnacles and bivalves. Their larvae attach and undergo metamorphosis into adults, leading to severe macrofouling problems [18].

The formation of biofilms often exhibits overlapping multi-stage characteristics rather than a simple linear sequence. Different fouling species exhibit considerable variability in the time required to establish stable adhesion on material surfaces, and no standardized timeline has been universally defined [19]. Photocatalytic antifouling technology provides a comprehensive, root-level solution to the multi-stage process of biofouling. Its fundamental mechanism relies on harnessing light energy to generate strong oxidizing agents, particularly reactive oxygen species (ROS). At the initial stage of fouling (conditioned film formation), ROS directly decompose adsorbed organic molecules, disrupting the “fertile ground” for microbial attachment. During subsequent microbial attachment and biofilm development stages, ROS effectively eliminate pioneer microorganisms like bacteria and diatoms while degrading their secreted extracellular polymers (EPS), thereby impeding biofilm maturation and stabilization. By preventing the establishment of stable microbial communities, this approach disrupts the chemical and biological cues necessary for the settlement of larval stages of larger fouling organisms such as barnacles, ultimately blocking the onset of macrofouling [20].

3. PRINCIPLES OF PHOTOCATALYTIC FOULING PREVENTION

Photocatalytic technology has emerged as a frontier research area due to its remarkable potential in energy conversion and environmental pollution control. Compared to traditional antifouling methods, this technology offers unique advantages such as environmental friendliness, sustainability, and high efficiency, garnering extensive attention from both academia and industry over the past decade. In antifouling coating applications, solar-driven photocatalytic materials can initiate surface reactions that alter hydrophilicity. Within photocatalytic antifouling systems, synergistic protection is achieved by combining physical barriers with photocatalytic activity. The central mechanism involves the formation of a dense hydration layer, generated through light-induced superhydrophilicity, which effectively prevents direct interaction between organic matter or microorganisms and the surface, thereby inhibiting fouling at its origin. At the same time, this hydration layer penetrates beneath pollutants undergoing photocatalytic breakdown, enabling water flow to carry away the degraded residues and creating a robust self-cleaning effect. This dual mechanism not only improves immediate antifouling performance but also sustains long-term photocatalytic efficiency by preventing the buildup of dead microbial debris—establishing a combined “chemical degradation + physical barrier” protection strategy [21].

The fundamental principles of photocatalysis involve the separation of photo-generated charges on the surface of semiconductor materials and the subsequent catalytic reaction process [22], typically encompassing five key stages, as illustrated in Figure **3**:

1. Light excitation: The sun on the left side of the diagram represents incident light. Process (1) indicates that after the photocatalyst absorbs a photon, an electron in the valence band (VB) gains energy and is excited to the conduction band (CB), simultaneously leaving a hole (h^+) in the valence band;

2. Charge separation: Process (2) demonstrates the separation of electrons (e^-) excited to the conduction band and holes (h^+) in the valence band. Electrons migrate toward the photocatalyst surface, while holes migrate toward the surface or bulk phase;

3. Carrier Migration: In step (3), the separated electrons (e^-) and holes (h^+) migrate toward the co-catalyst on the photocatalyst surface, preparing for subsequent surface reactions;

4. Carrier recombination: ① Surface recombination: As indicated by the orange arrow in process (4), some electrons and holes that

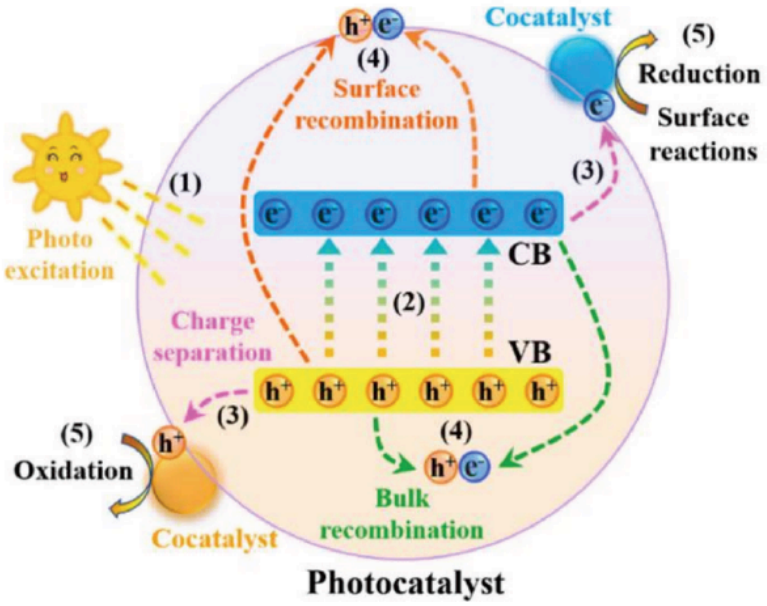

Figure 3: Schematic Diagram of the Photocatalytic Reaction Process: "From Light Energy to Chemical Energy" [22].

migrate to the surface recombine, resulting in energy loss; ② Bulk recombination: As indicated by the green arrow in process (4), electrons and holes also recombine within the bulk of the photocatalyst, similarly causing energy loss;

5. Surface Reactions: ① Oxidation Reaction: Holes (h^+) on the left-side co-catalyst participate in the oxidation reaction, oxidizing the reactants; ② Reduction Reaction: Electrons (e^-) on the right-side co-catalyst participate in the reduction reaction, reducing the reactants.

Through these steps, semiconductor materials can catalyze water splitting or other chemical reactions under illumination, enabling applications in environmental remediation and energy conversion. Steps (3) and (4) are critical for determining overall catalytic performance. Therefore, contemporary research efforts are predominantly directed toward addressing the central challenge of promoting efficient charge separation while concurrently suppressing recombination losses [23].

Semiconductors possess distinctive electrical properties, exhibiting conductivity between metals (10^4–10^6 S/cm) and insulators (<10^{-6} S/cm). Their electronic band structure is characterized by a bandgap, across which electrons can be excited from the valence band to the conduction band under light irradiation. This transition generates electron–hole pairs (e^--h^+), which serve as the basis for redox activity in photocatalytic processes. Upon photoexcitation, semiconductor photocatalysts facilitate surface reactions that decompose seawater and dissolved oxygen to generate multiple reactive oxygen species (ROS), including superoxide radicals ($\bullet O_2^-$), singlet oxygen ($^1O_2$), and hydroxyl radicals (•OH) [24].

Liu *et al*. [25] developed an atomically strained In_2S_3/MBene photocatalyst capable of efficiently activating oxygen to generate superoxide radicals ($\bullet O_2^-$) in low dissolved oxygen environments, achieving a 16.59-fold increase in yield. The photocatalytic disinfection system constructed based on this material operates stably, demonstrating disinfection capabilities nearly 25 times superior to commercial sodium hypochlorite, showcasing significant practical application potential. Jian Wang *et al*. [26] developed a floating monolithic photocatalyst (AgSA+NP/ZIF) loaded with silver single atoms and nanoparticles. Silver single atoms promote reactive oxygen species (ROS) generation, while the photothermal effect of silver nanoparticles weakens bacterial resistance. Through synergistic action, this catalyst achieves ultra-efficient inactivation of highly resistant enterobacteria exceeding 99.9999% within 30 minutes, with disinfected water output meeting WHO standards. These ROS undergo intense oxidative reactions with key components of bacterial cell membranes such as lipids, polysaccharides, and proteins—leading to membrane structural disruption and bacterial death [27]. Based on this mechanism, photocatalytic technology effectively degrades organic pollutants adhering to material surfaces, thereby inhibiting the fouling process of marine organisms [28]. Furthermore, these ROS can degrade the extracellular polymeric substances (EPS) secreted by marine organisms during attachment, making it difficult for fouling organisms to adhere to and form stable biofilms on coated surfaces. Additionally, some photocatalysts undergo hydrophilicity changes

during photocatalysis, rendering the coating surface more hydrophilic and thereby inhibiting marine organism attachment from a physical antifouling perspective.

4. TYPES OF PHOTOCATALYSTS

Common semiconductor materials employed in photo catalysis include titanium dioxide (TiO_2), zinc oxide (ZnO), cadmium sulfide (CdS), and modified carbon nitride (g-C_3N_4). These materials possess unique electronic band structure characteristics [29-32], where the valence band (VB) is filled with electrons while the conduction band (CB) remains vacant, separated by a bandgap. This distinct band arrangement enables these materials to generate efficient electron-hole pairs under illumination, thereby exhibiting outstanding photocatalytic activity. Although titanium dioxide (TiO_2) and zinc oxide (ZnO) photocatalysts exhibit good chemical stability and anti-fouling properties under ultraviolet light, they have low visible light utilization rates [33]. Current research on photocatalytic coatings primarily focuses on enhancing the photocatalytic activity of photocatalysts and improving their utilization of visible light.

4.1. Metal Oxide Photocatalysts

Metal oxides, characterized by high chemical stability, relatively low cost, and ease of preparation, represent a widely studied and applied class of photocatalysts [34]. In recent years, research on metal oxide photocatalysts such as titanium dioxide (TiO_2), zinc oxide (ZnO), and cerium dioxide (CeO_2) for marine antifouling coatings has focused on enhancing photocatalytic efficiency, broadening spectral response ranges, and improving environmental adaptability. Through diverse approaches including heterostructure construction, green synthesis, elemental doping, and smart response system design, researchers are continuously improving their bactericidal performance and practicality in marine antifouling coatings. These strategies collectively propel the development of such photocatalytic antifouling technologies toward high efficiency, long-lasting performance, and environmental friendliness [35].

Drunka *et al*. [36] enhanced the photocatalytic performance of TiO_2 nanofibers through a synergistic noble metal co-doping strategy. By incorporating gold (Au), platinum (Pt), and silver (Ag) into the TiO_2 matrix, they significantly improved the material's photocatalytic efficiency. Catalytic performance was evaluated via visible-light-driven methylene blue degradation experiments. Results showed that after 60 min of visible light irradiation, the TiO_2 nanofiber composites doped with 1% Au/Pt/Ag achieved methylene blue degradation efficiencies of 97.5% (Au), 86.2% (Pt), and 70.4% (Ag), respectively, demonstrating significantly enhanced catalytic performance compared to undoped TiO_2 nanofibers. Fatemeh Hedayati Tabari *et al*. [37] successfully synthesized TiO_2/ZnO composite nanofibers with varying ratios via electrospinning. They verified the formation of direct Z-type heterojunction photocatalysts through computational band alignment analysis and further confirmed this via active species trapping experiments. Through comprehensive investigation of factors influencing photocatalytic activity, TiO_2/ZnO nanofibers with an electrospun ratio of 1:4 exhibited outstanding photocatalytic performance: under optimal conditions, they achieved a remarkable 97.26% removal efficiency for Rhodamine B (RhB) in aqueous solution. After 60 minutes of UV irradiation, the mineralization efficiency based on total organic carbon (TOC) analysis reached 84.18%. Antimicrobial evaluation further revealed synergistic effects, with TiO_2/ZnO 1:4 nanofibers exhibiting significantly enhanced antibacterial efficacy against Staphylococcus aureus and Escherichia coli. Sajedeh Mazarei *et al*. [38] synthesized zinc oxide nanoparticles using a green method involving mangrove plants. After 48 hours of antibacterial testing, the minimum inhibitory concentrations (MIC) of the zinc oxide nanoparticles against Staphylococcus aureus and Escherichia coli were 6.25 mg/L and 25 mg/L, respectively. At a concentration of 800 mg/L, the zinc oxide nanoparticles inhibited the growth rates of Spirulina, Dunaliella salina, and Muelleria filamentosa by 90.88%, 94.06%, and 92.49%, respectively, demonstrating their high potential for effective inhibition. Dan Su *et al*. [39] synthesized cerium oxide nanoparticles (CeO_2NPs) on the surface of dopamine-modified 5083 aluminum alloy by mimicking the chemical principles of mussels. This method enables full exposure of CeO_2NPs on the coating surface, and the CeO_2 nanocoating exhibits peroxidase-like activity. This nanocoating demonstrated outstanding fouling inhibition against Mytilus edulis, Escherichia coli, and Bacillus species, reducing fouling levels by 96.03%, 94.41%, and 88.44%, respectively. Shaban *et al*. [40] successfully synthesized Ni-doped and Ni/Cr co-doped TiO_2 nanotube materials via hydrothermal synthesis. Figure **4** illustrates the charge transfer pathway of the 6Ni-4Cr/TiO_2 photocatalyst during the reaction process. In methylene blue photocatalytic degradation experiments, Ni doping caused a blue shift (approximately 15 nm) in the TiO_2 absorption edge, while Ni/Cr co-doping induced a pronounced red shift (approximately 32 nm). The 6Ni/4Cr co-doped TiO_2 nanotubes exhibited the most outstanding photocatalytic performance, achieving a degradation efficiency of 95.6% for methylene blue under standard

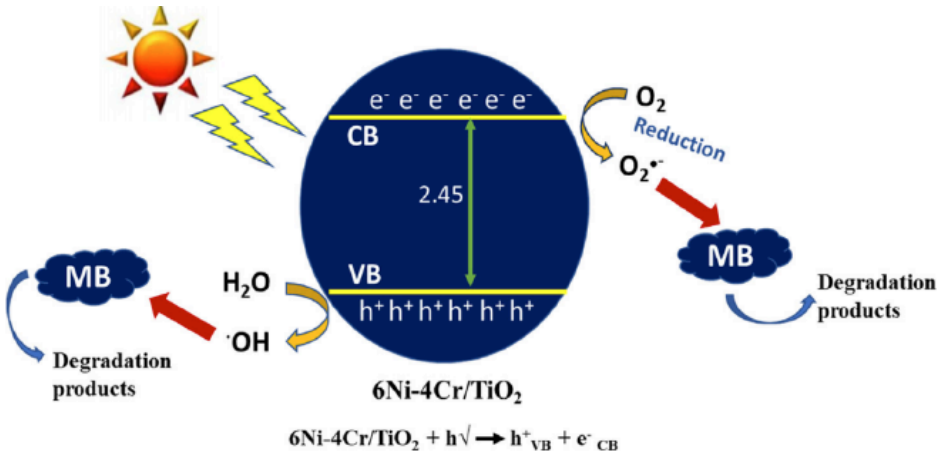

Figure 4: Schematic illustration of charge transfer route in the 6Ni-4Cr/TiO_2 based photocatalyst [40].

test conditions. This study confirms that noble metal doping can effectively extend the optical response range of TiO_2 into the visible light region and enhance the separation efficiency of photo-generated carriers through surface plasmon resonance (SPR) effects.

4.2. Sulfide Photocatalysts

Sulfide semiconductors (*e.g.*, CdS, ZnS) exhibit significant advantages in photocatalysis due to their unique electronic structure characteristics. In the field of marine antifouling coatings, the application of sulfide photocatalysts remains in the exploratory stage. Among these, cadmium sulfide (CdS) stands out as the most promising candidate material due to its unique performance advantages. This material possesses a narrow bandgap width, exhibiting high compatibility with the near-ultraviolet to visible light region of the solar spectrum. This enables it to efficiently utilize natural light sources for photocatalytic activity. Studies have shown that CdS-based coatings exhibit dual anti-fouling functions in marine environments: they achieve efficient sterilization through ROS generated by photocatalysis while simultaneously degrading organic fouling substances, thereby effectively inhibiting the attachment and growth of marine organisms such as barnacles and algae [41].

Ren *et al*. [42] innovatively developed an S-type heterojunction CdS photocatalytic system. By compositing CdS with oxidizing semiconductors such as CeO_2 and WO_3, they achieved a significant enhancement in photocatalytic performance. This study further presents a promising strategy to address the critical issue of Cd^{2+} ion leaching toxicity in CdS-based materials for marine applications. The system enhances the controlled migration and separation of photogenerated carriers through a triple synergistic mechanism involving the built-in electric field at the heterojunction interface, band bending effects, and electrostatic interactions. Taking the SnS_2/CdS system as an example, its hydrogen production rate surpassed that of the single-component system. Meanwhile, the CdS/WO_3 composite simultaneously retained strong reducing power of CdS and strong oxidizing power of WO_3, resulting in extended carrier lifetime. This research offers novel insights for addressing critical issues such as high carrier recombination rates and poor stability in CdS-based materials. It also demonstrates outstanding stability in tests simulating marine environments. Building on this progress, Guo *et al*. [43] successfully synthesized a CdS/CoP composite photocatalyst with gradient phosphorus doping characteristics by phosphorization treatment using CdS/$Co(OH)_2$ as the precursor. This material exhibits a significant bandgap tuning effect. The intrinsic bandgap of pristine CdS is 2.45 eV, while the bandgap of the composite material can be tuned to 1.90 eV after gradient phosphorus doping modification, achieving bandgap narrowing. This bandgap engineering strategy enables a stepwise enhancement in the material's light absorption performance. Sun *et al*. [44] synthesized the ternary composite PdS/CdS/MoS_2 using microwave-assisted synthesis. Due to dual co-catalyst loading, photo-generated electrons and holes in CdS can be transferred to MoS_2 and PdS, respectively. The introduction of PdS enables timely extraction of photo-generated holes from CdS, effectively suppressing CdS photocorrosion. In another approach, Lei *et al*. [45] synthesized CdS/MoC composite photocatalysts via physical mixing under ambient conditions. MoC acts as a co-catalyst to capture photo-generated electrons while suppressing photo-generated carrier recombination, thereby enhancing photocatalytic hydrogen production activity. Gao *et al*. [46] employed a solvothermal method to prepare a composite photocatalytic material consisting of $Zn_{0.5}Cd_{0.5}S$ nanoparticles/ultrathin $Ni(OH)_2$ nanosheets. This system achieved multiple

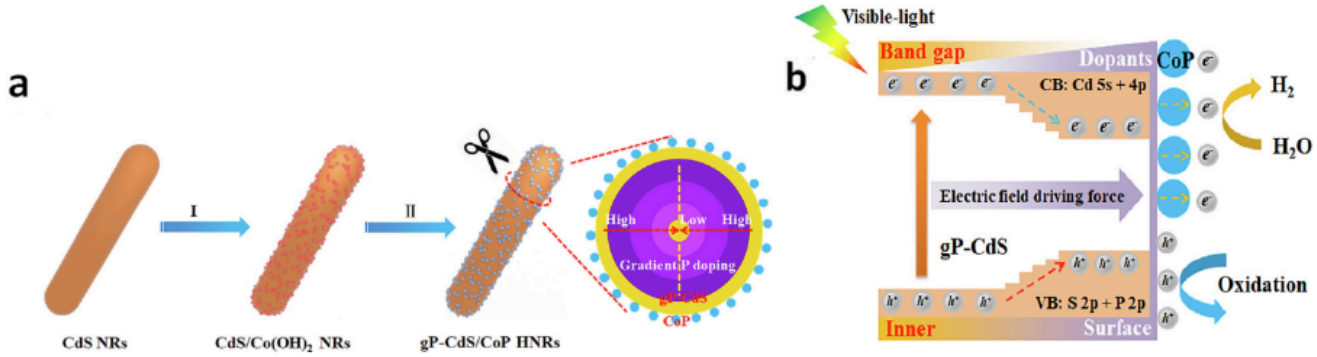

Figure 5: (**a**) Schematic illustration of the synthetic process of the *g*P-CdS/CoP HNRs, (**b**) Schematic illustration of the charge transfer mechanism in *g*P-CdS/CoP HNRs under visible light irradiation [43].

performance enhancements by constructing a tightly integrated heterojunction interface. The ultrathin $Ni(OH)_2$ nanosheets function as an efficient non-precious metal co-catalyst to promote photo-induced electron transfer while providing a uniformly dispersed substrate for the $Zn_{0.5}Cd_{0.5}S$ nanoparticles. This synergistic effect significantly enhances the photocatalytic hydrogen production activity compared to single-component systems and reduces the overpotential.

4.3. Nitride Photocatalysts

Nitride-based photocatalysts, especially graphitic carbon nitride (g-C_3N_4) and its modified derivatives, have attracted growing interest in marine antifouling coating research due to their visible-light responsiveness, strong antibacterial performance, and environmentally friendly nature. Among them, g-C_3N_4 has become a focal material thanks to its graphene-like two-dimensional layered structure, suitable visible-light bandgap (~2.7 eV), and metal-free composition that avoids secondary environmental risks. By employing strategies such as elemental doping (*e.g.*, phosphorus, sulfur), constructing heterojunctions (*e.g.*, with COF or BiOBr composites), or tailoring microstructures (*e.g.*, porous frameworks or ultrathin layers), its charge separation efficiency can be markedly improved while extending the light absorption range. These modifications enable the efficient production of reactive oxygen species under simulated marine illumination, thereby effectively suppressing biofilm formation by bacteria, diatoms, and microalgae.

Wang *et al*. [47] synthesized *g*-C_3N_4@TiO_2 core-shell photocatalysts with controllable shell thicknesses (0 nm, 1.0 nm, 1.5 nm, 3.0 nm) via an in-situ coating and reassembly sol-gel method, addressing the challenges of difficult layer control and weak core-shell bonding in conventional physical coating methods. The 1.0 nm shell layer (annealed at 550°C) exhibited optimal performance, demonstrating visible-light phenol degradation activity 7.2 times higher than bulk *g*-C_3N_4. Its photocurrent, phenol removal rate (30%), and mineralization degree (19.8%) significantly surpassed those of individual materials. The electron-hole separation process of the *g*-C_3N_4@TiO_2 core-shell photocatalyst under visible light irradiation is illustrated as shown in Figure **6**. Furthermore, the catalyst is stable, easily recoverable, and free from secondary pollution. Building on material modification strategies. Zhang *et al*. [48] explored a novel photocatalytic method for inactivating Aurelia coerulea hydras by synthesizing P-g-C_3N_4 photocatalysts doped with trace amounts of Ag_2O. During photocatalytic reactions, the Ag_2O@P-g-C_3N_4 composite containing 1.11% silver induced mortality in up to 84.6% of jellyfish larvae under weak visible light irradiation (simulating natural habitats). This photocatalyst exhibits high electron density and photostability, simultaneously enhancing visible light capture efficiency while reducing photo-generated electron-hole recombination rates.Wu *et al*. [49] flexibly constructed three types of covalent organic framework (COF) nanotubes/two-dimensional nanosheet heterojunctions (COF-x) on g-C_3N_4, WSe_2, and $Ti_3C_2T_x$ nanosheet substrates via an in-situ growth method using a one-pot approach. The internal electric field generated at the COF-x coupling interface enhances the separation and migration of photogenerated charge pairs, promoting the generation of antibacterial reactive oxygen species (ROS) by COF-x. This results in an efficiency increase of 2.8 to 270 times compared to nanosheets. At an ultra-low concentration of 2 μg/mL and weak visible light irradiation of 15 mW/cm^2, the bactericidal rate of COF-x increased from 34.13%-41.68% for pure nanosheets to over 99.86%. At a low concentration of 20 μg/mL, COF-x achieved nearly 100% bactericidal efficacy within 6 hours. This material demonstrates outstanding environmental stability and antibacterial performance under thermal, photochemical, acidic/alkaline, and aqueous conditions, opening new perspectives in the field of photocatalytic antibacterial/antifouling applications. Ge *et al*. [50] designed a novel GaSe/ZrS_2 direct Z-type

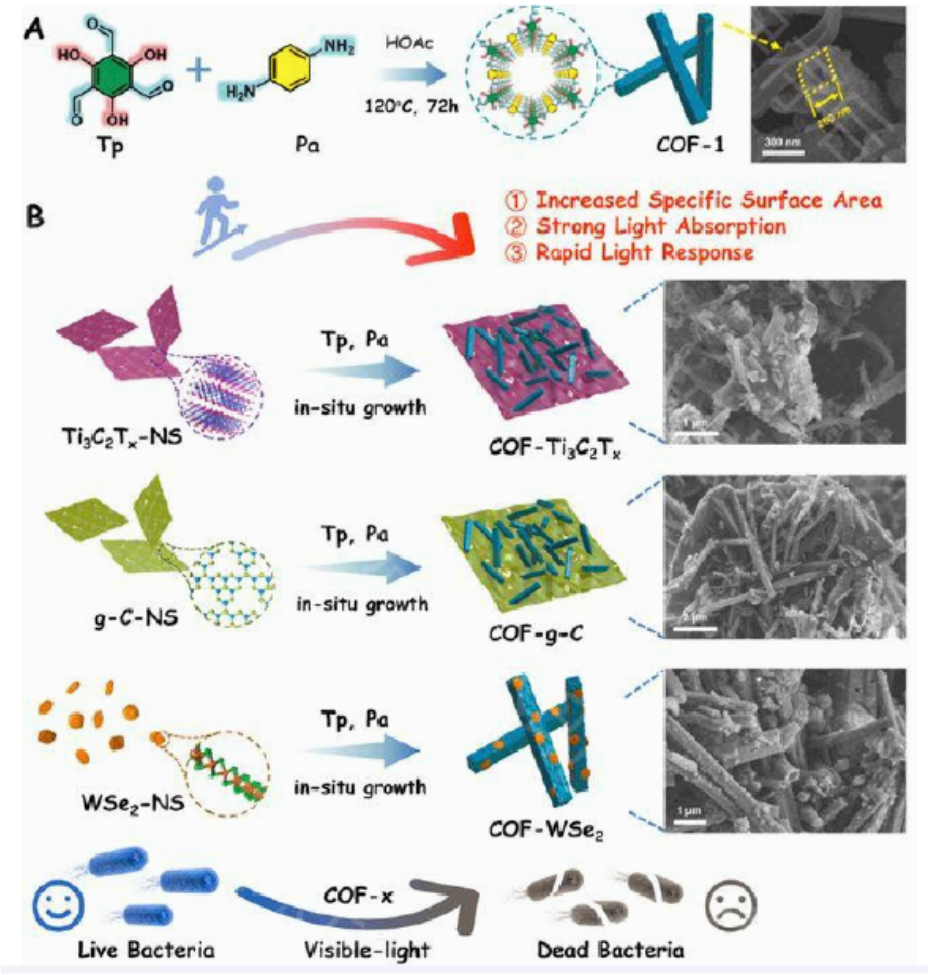

Figure 6: Schematic of the Synthesis of COF Nanotube/2D Nanoplate Heterostructures (COF-x) [49].

heterojunction photocatalyst. This material achieves multiple performance breakthroughs through a unique Z-type charge transport mechanism: First, the built-in interfacial electric field promotes efficient spatial separation of photogenerated carriers, extending carrier lifetime compared to single-component systems; Second, the system simultaneously retains high reduction potential of GaSe and strong oxidation potential of ZrS_2. Importantly, this composite also demonstrated excellent structural and photocatalytic stability, underscoring its potential for long-term application.

4.4. Other Photocatalysts

In recent years, the development of advanced photocatalysts has increasingly emphasized functionalization and hybridization. This trend aims to address the inherent shortcomings of single semiconductor materials such as TiO_2 and ZnO, which are often limited by rapid recombination of photogenerated electron–hole pairs and their reliance on ultraviolet light. To overcome these challenges, researchers are adopting composite and hybrid design strategies. Approaches such as coupling with two-dimensional materials (*e.g.*, MXenes) and integrating metal–organic frameworks (MOFs) have been widely explored. These methods effectively extend light absorption into the visible range, suppress electron–hole recombination, and introduce additional surface active sites, thereby enhancing the overall photocatalytic efficiency for antifouling applications.

As an emerging two-dimensional conductive material, MXene has exceptionally high electron mobility, making it an ideal “electronic highway”. When combined with semiconductors, it significantly enhances the separation and transport of photo-generated charges, effectively resolving the core challenge of charge recombination inherent in traditional photocatalysts. Masoud Akbari *et al*. [51] successfully synthesized Fe_2O_3-SiO_2/MXene ternary nanophotocomposites via wet impregnation and sonochemical methods, and optimized their photocatalytic degradation performance of tetracycline in water using response surface methodology. Results indicate that under optimal conditions (Fe_2O_3-SiO_2 loading 25 wt%, calcination temperature 450 ℃, catalyst dosage 0.75 g/L, pH=5.57, irradiation time 68.28 min), the Fe_2O_3-SiO_2/MXene composite

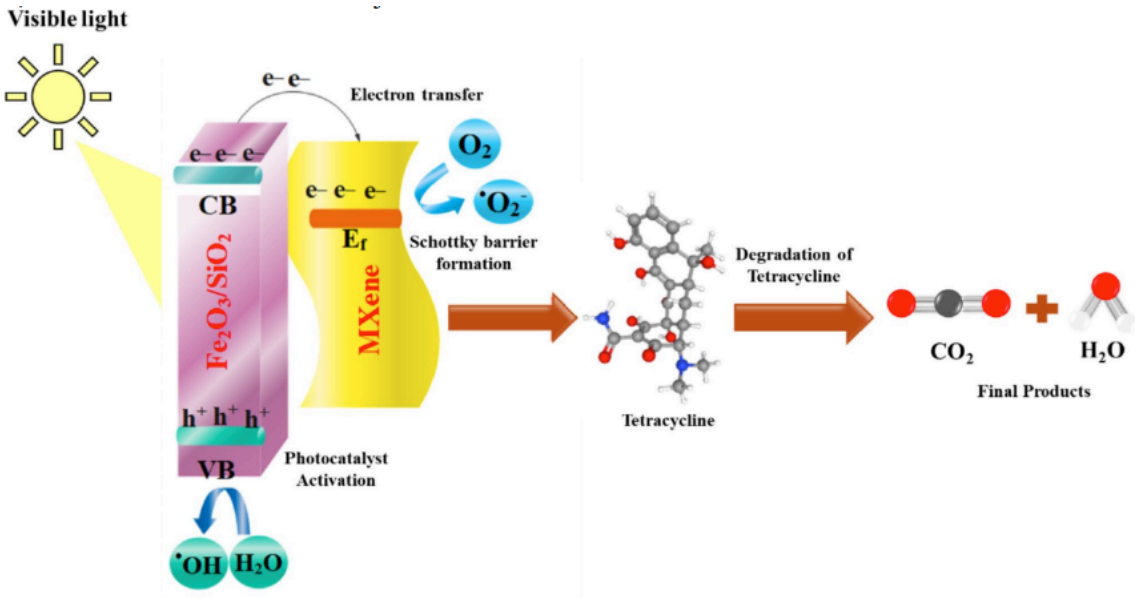

Figure 7: Proposed charge transfer mechanism of the 25FeS/MX-450 photocatalyst under visible light exposure [51].

achieved a degradation rate of 98% for tetracycline. MOFs excel with their remarkable specific surface area and precisely tunable pore architecture, offering not only abundant reaction sites but also enabling the "customization" of band structures through the regulation of organic ligands and metal centers. This provides a platform for achieving highly efficient and selective photocatalysis. Jun Yuan *et al*. [52] successfully synthesized a hollow-structured Ce-MOF@h-CeO_2 composite photocatalyst. By integrating Ce-MOF with hollow cerium dioxide (h-CeO_2), they significantly enhanced photocatalytic performance under visible light. This composite demonstrated outstanding activity in degrading Rhodamine B (RhB) and photocatalytically producing hydrogen from water, exhibiting degradation efficiencies 7.17-fold and 4.46-fold higher than pure h-CeO_2 and Ce-MOF, respectively, with a hydrogen production rate reaching 3419.38 $\mu mol \cdot g^{-1} \cdot h^{-1}$. The performance enhancement is attributed to the abundant reaction sites provided by the hollow structure, charge transport facilitated by π-π conjugated ligands, and the effective suppression of electron-hole pair recombination by the heterojunction structure. Bismuth-based materials (such as $BiVO_4$ and Bi_2WO_6) excel due to their inherent sensitivity to visible light and environmental friendliness. Their unique layered structure facilitates the migration of photo-generated charge carriers. Zhang *et al*. [53] successfully synthesized three-dimensional porous BiOI/Ti_3C_2 nanocomposites via a solvothermal method. This material exhibits a mesoporous structure with pore sizes ranging from 2.5 to 20 nm, providing abundant active sites for photocatalytic reactions. In another study, Li *et al*. [54] precisely controlled the reactant ratio to synthesize a ternary photocatalyst (MB-0.05) composed of graphitic carbon-doped α-Bi_2O_3/β-Bi_2O_3/Bi_5O_7I with a double S-type heterojunction structure. This material demonstrated outstanding photocatalytic degradation performance for bisphenol A (BPA) under simulated sunlight conditions. Liu *et al*. [55] successfully prepared a $BiVO_4$/BiOBr composite photocatalyst via in situ chemical transformation, significantly enhancing photocatalytic activity. This study employed hydrobromic acid (HBr) as a structural regulator, enabling uniform growth of BiOBr nanosheets on the $BiVO_4$ surface to form a dense heterojunction interface.

5. CONCLUSION

Photocatalytic marine antifouling technology has emerged as one of the most promising alternatives to traditional antifouling coatings due to its environmental friendliness, low energy consumption, and long-lasting anti-fouling properties. However, single photocatalysts commonly suffer from issues such as low visible light utilization, easy carrier recombination, insufficient physicochemical stability, and weak adhesion to substrates, limiting their large-scale practical application. Research on photocatalytic marine antifouling coatings has increasingly emphasized enhancing both performance and environmental compatibility through multi-component synergistic approaches in recent years. This strategy focuses on integrating highly efficient photocatalysts (*e.g.*, TiO_2, g-C_3N_4) with functional nanocomposites (such as noble metal/semiconductor heterojunctions or carbon nanomaterial composites) and degradable or stimuli-responsive polymers (*e.g.*, polycaprolactone, poly(N-isopropylacrylamide)). Such combinations pave the way for "intelligent" antifouling interfaces capable of

adaptive fouling recognition, controlled and prolonged ROS release, and surface self-renewal. By systematically integrating advanced photocatalytic materials, multifunctional nanocomposite units, and intelligent polymer matrices, we can ultimately achieve “green, efficient, long-lasting, and intelligent” marine antifouling coatings.

ACKNOWLEDGMENT

This work was supported by the National Key Research and Development Program of China (2022YFB3704700, 2022YFB3704702)), the Major Scientific and Technological Innovation Project of Shandong Province (Grant No. 2021CXGC010901), Taishan Scholar Program of Shandong Province (Grant No. TS201511031), and Taishan Industrial Experts Program of Shandong Province. (No. tsls20241105).

AUTHORS STATEMENT

The author declares that there is no conflict of interest between the authors or between the authors and the projects sponsors.

REFERENCES

[1] Habibi H, Gan T H. An acoustic antifouling study in sea environment for ship hulls using ultrasonic guided waves [J]. International Journal of Engineering Technologies and Management Research, 2016, 3(4): 14-30. https://doi.org/10.29121/IJETMR.V3.I4.2016.59

[2] Cao S, Wang J D, Chen H S, *et al*. Progress of marine biofouling and antifouling technologies [J]. Chinese Science Bulletin, 2011, 56: 598-612. https://doi.org/10.1007/s11434-010-4158-4

[3] Korkut E, Atlar M. An experimental investigation of the effect of foul release coating application on performance, noise and cavitation characteristics of marine propellers [J]. Ocean Engineering, 2012, 41: 1-12. https://doi.org/10.1016/j.oceaneng.2011.12.012

[4] Guo M, Chen Z, Song M, *et al*. Multifamily nanozymes for sustainable and eco-friendly marine antifouling [J]. Nano Letters, 2025, 25(12): 4878-4886. https://doi.org/10.1021/acs.nanolett.4c06675

[5] Figueiredo J, Oliveira T, Ferreira V, *et al*. Toxicity of innovative anti-fouling nano-based solutions to marine species [J]. Environmental Science: Nano, 2019, 6(5): 1418-1429. https://doi.org/10.1039/C9EN00011A

[6] Schultz M P. Effects of coating roughness and biofouling on ship resistance and powering [J]. Biofouling, 2007, 23(5): 331-341. https://doi.org/10.1080/08927010701461974

[7] Demirel Y K, Uzun D, Zhang Y, *et al*. Effect of barnacle fouling on ship resistance and powering [J]. Biofouling, 2017, 33(10): 819-834. https://doi.org/10.1080/08927014.2017.1373279

[8] Georgopoulou C, Di Maria C, Di Ilio G, *et al*. On the identification of regulatory gaps for hydrogen as maritime fuel [J]. Sustainable Energy Technologies and Assessments, 2025, 75: 104224. https://doi.org/10.1016/j.seta.2025.104224

[9] Liu M, Ma W, Zhang M, *et al*. Bio-inspired design of antifouling polymeric coatings with natural extracts: key evidence for resistance to fouling adhesion [J]. Advanced Composites and Hybrid Materials, 2025, 8(1): 139. https://doi.org/10.1007/s42114-024-01094-z

[10] Guan X, Zhu P, Ullah Z, *et al*. CrB-based triboelectric nanogenerator with ultrahigh current output for electrical antifouling [J]. Chemical Engineering Journal, 2025, 522:168262 https://doi.org/10.1016/j.cej.2025.168262

[11] Zhu P, Ullah Z, Zheng S, *et al*. Ultrahigh current output from triboelectric nanogenerators based on UIO-66 materials for electrochemical cathodic protection [J], 2023,108:108195. https://doi.org/10.1016/j.nanoen.2023.108195

[12] Zhang X, Zhang J, Yu J, *et al*. Fabrication of $InVO_4/AgVO_3$heterojunctions with enhanced photocatalytic antifouling efficiency under visible-light [J]. Applied Catalysis B: Environmental, 2018, 220: 57-66. https://doi.org/10.1016/j.apcatb.2017.07.074

[13] Ou C, Chen J, Li Y, *et al*. Valence-invariable catalysis-mediated generation of reactive oxygen species and subsequent photothermal-triggered release of alkyl radicals via a Zr-based metal-organic framework nanohybrid for programmed multi-mode antibiofilm therapy[J]. Chemical Engineering Journal, 2025: 164870. https://doi.org/10.1016/j.cej.2025.164870

[14] Liu Z, Zheng X, Zhang H, *et al*. Review on formation of biofouling in the marine environment and functionalization of new marine antifouling coatings [J]. Journal of Materials Science, 2022, 57(39): 18221-18242. https://doi.org/10.1007/s10853-022-07791-8

[15] Qian P Y, Cheng A, Wang R, *et al*. Marine biofilms: diversity, interactions and biofouling [J]. Nature Reviews Microbiology, 2022, 20(11): 671-684. https://doi.org/10.1038/s41579-022-00744-7

[16] Bian S, Wang Y, Yao C, *et al*. Inducing the formation of organic-inorganic carbonated composites via extracellular polymeric substances (EPS)-modified carbonation in low-calcium CO_2 sequestration materials[J]. Cement and Concrete Composites, 2025: 106277. https://doi.org/10.1016/j.cemconcomp.2025.106277

[17] Chen Y, Ye H, Zhao X, *et al*. Strategy for fabricating degradable low-surface-energy cross-linked networks with excellent anti-fouling properties [J]. ACS Applied Materials & Interfaces, 2025, 17(2): 3995-4008. https://doi.org/10.1021/acsami.4c19192

[18] Jin H, Tian L, Bing W, *et al*. Bioinspired marine antifouling coatings: Status, prospects, and future [J]. Progress in Materials Science, 2022, 124: 100889. https://doi.org/10.1016/j.pmatsci.2021.100889

[19] Liu M, Li S, Wang H, *et al*. Research progress of environmentally friendly marine antifouling coatings [J]. Polymer Chemistry, 2021, 12(26): 3702-3720. https://doi.org/10.1039/D1PY00512J

[20] Liu Q, Wang Z. Reactive oxygen species generation by organic materials for efficient photocatalysis [J]. Chinese Chemical Letters, 2025: 111504. https://doi.org/10.1016/j.cclet.2025.111504

[21] Zhou A, Sand W, Wang X, *et al*. Self-growing composite photocatalytic materials for surface self-renewal of marine antifouling coatings [J]. Separation and Purification Technology, 2025, 354: 129387. https://doi.org/10.1016/j.seppur.2024.129387

[22] Wang Q, Zhou Y, Zhang K, *et al*. Defect-enrichment in porous interface of ultrathin CuO nanobelts realizes a novel CO_2 photoreduction pathway [J]. Journal of Materials Chemistry A, 2023, 11(16): 8776-8782. https://doi.org/10.1039/D3TA00824J

[23] Shandilya P, Sambyal S, Sharma R, *et al*. Properties, optimized morphologies, and advanced strategies for photocatalytic applications of WO_3-based photocatalysts [J]. Journal of Hazardous Materials, 2022, 428: 128218. https://doi.org/10.1016/j.jhazmat.2022.128218

[24] Wang R, Yu W, Fang N, *et al*. Constructing fast charge separation of $ZnIn_2S_4$@$CuCo_2S_4$ pn heterojunction for efficient photocatalytic hydrogen energy recovery from quinolone antibiotic wastewater [J]. Applied Catalysis B:

Environmental, 2024, 341: 123284.
https://doi.org/10.1016/j.apcatb.2023.123284

[25] Liu Z, Gao W, Liu L, *et al*. Spin polarization induced by atomic strain of MBene promotes the· O^{2-} production for groundwater disinfection [J]. Nature Communications, 2025, 16(1): 197.
https://doi.org/10.1038/s41467-024-55626-8

[26] Wang J, Zhang J, Li Y, *et al*. Silver single atoms and nanoparticles on floatable monolithic photocatalysts for synergistic solar water disinfection [J]. Nature communications, 2025, 16(1): 981.
https://doi.org/10.1038/s41467-025-56339-2

[27] Liang Y, Xu W, Fang J, *et al*. Highly dispersed bismuth oxide quantum dots/graphite carbon nitride nanosheets heterojunctions for visible light photocatalytic redox degradation of environmental pollutants [J]. Applied Catalysis B: Environmental, 2021, 295: 120279.
https://doi.org/10.1016/j.apcatb.2021.120279

[28] Xong G, Zhang Z, Zhang C, *et al*. SLAP@g-C_3N_4 fluorescent photocatalytic composite powders enhance the anti-bacteria adhesion performance and mechanism of polydimethylsiloxane coatings [J]. Nanomaterials, 2022, 12(17): 3005.
https://doi.org/10.3390/nano12173005

[29] Gu Y, Yu L, Mou J, *et al*. Research strategies to develop environmentally friendly marine antifouling coatings [J]. Marine Drugs, 2020, 18(7): 371.
https://doi.org/10.3390/md18070371

[30] Zhou C, Lai C, Zhang C, *et al*. Semiconductor/boron nitride composites: Synthesis, properties, and photocatalysis applications [J]. Applied Catalysis B: Environmental, 2018, 238: 6-18.
https://doi.org/10.1016/j.apcatb.2018.07.011

[31] Liu X, Huang B, Li J, *et al*. Full-spectrum plasmonic semiconductors for photocatalysis [J]. Materials Horizons, 2024, 11(22): 5470-5498.
https://doi.org/10.1039/D4MH00515E

[32] Huang F, Zhang F, Wang Y, *et al*. Semiconductor cooperative photocatalysis with TEMPO [J]. Trends in Chemistry, 2024, 6(3): 115-127.
https://doi.org/10.1016/j.trechm.2024.01.002

[33] Yu Y, Ming H, He D, *et al*. V_2O_5-based photocatalysts for environmental improvement: key challenges and advancements [J]. Journal of Environmental Chemical Engineering, 2023, 11(6): 111243.
https://doi.org/10.1016/j.jece.2023.111243

[34] Zhou X, Hwang I, Tomanec O, *et al*. Advanced photocatalysts: pinning single atom co-catalysts on titania nanotubes [J]. Advanced Functional Materials, 2021, 31(30): 2102843.
https://doi.org/10.1002/adfm.202102843

[35] Ly H N, Parasuraman V, Han T U, *et al*. Enhanced removal of volatile organic compounds and bacterial disinfection using silver-integrated urchin-like porous titanium dioxide as a multifunctional photocatalyst [J]. Journal of Cleaner Production, 2025, 497: 145153.
https://doi.org/10.1016/j.jclepro.2025.145153

[36] Drunka R, Grabis J, Krumina A. Preparation of Au, Pt, Pd and Ag doped TiO_2 nanofibers and their photocatalytic properties under LED illumination [J]. Key Engineering Materials, 2018, 762: 283-287.
https://doi.org/10.4028/www.scientific.net/KEM.762.283

[37] Tabari F H, Hamidinezhad H. Effective photodegradation of organic pollutants and antibacterial activity by TiO_2/ZnO composite nanofibers as a direct Z-scheme heterojunction photocatalyst [J]. Journal of Water Process Engineering, 2025, 77: 108562.
https://doi.org/10.1016/j.jwpe.2025.108562

[38] Mazarei S, Safaie M, Homaei A, *et al*. Progress in tailor-made of anti-fouling coating strategies for marine fish farming cages based on green synthesis of zinc oxide nanoparticles from Avicennia marina leaves [J]. Progress in Organic Coatings, 2025, 208: 109465.
https://doi.org/10.1016/j.porgcoat.2025.109465

[39] Su D, Liu Y, Chang J, *et al*. Improved Antifouling and Anticorrosion Performance of CeO_2 Nanocoating Prepared by Mussel-Inspired Chemistry [J]. Langmuir, 2025, 41(6): 3951-3960.
https://doi.org/10.1021/acs.langmuir.4c04151

[40] Shaban M, Ahmed A M, Shehata N, *et al*. Ni-doped and Ni/Cr co-doped TiO_2 nanotubes for enhancement of photocatalytic degradation of methylene blue [J]. Journal of Colloid and Interface Science, 2019, 555: 31-41.
https://doi.org/10.1016/j.jcis.2019.07.070

[41] Wang W, Xue J, Liu J. Recent advances in CdS heterojunctions: morphology, synthesis, performances and prospects [J]. Journal of Materials Chemistry A, 2024, 12(18): 10659-10675.
https://doi.org/10.1039/D4TA01260G

[42] Ren Y, Li Y, Pan G, *et al*. Recent progress in CdS-based S-scheme photocatalysts [J]. Journal of Materials Science & Technology, 2024, 171: 162-184.
https://doi.org/10.1016/j.jmst.2023.06.052

[43] Guo C, Li L, Chen F, *et al*. One-step phosphorization preparation of gradient-P-doped CdS/CoP hybrid nanorods having multiple channel charge separation for photocatalytic reduction of water [J]. Journal of Colloid and Interface Science, 2021, 596: 431-441.
https://doi.org/10.1016/j.jcis.2021.03.170

[44] Sun B, Zheng J, Yin D, *et al*. Dual cocatalyst modified CdS achieving enhanced photocatalytic H_2 generation and benzylamine oxidation performance [J]. Applied Surface Science, 2022, 592: 153277.
https://doi.org/10.1016/j.apsusc.2022.153277

[45] Lei Y, Wu X, Li S, *et al*. Noble-metal-free metallic MoC combined with CdS for enhanced visible-light-driven photocatalytic hydrogen evolution [J]. Journal of Cleaner Production, 2021, 322: 129018.
https://doi.org/10.1016/j.jclepro.2021.129018

[46] Gao X, Zeng D, Yang J, *et al*. Ultrathin $Ni(OH)_2$ nanosheets decorated with $Zn_{0.5}Cd_{0.5}S$ nanoparticles as 2D/0D heterojunctions for highly enhanced visible light-driven photocatalytic hydrogen evolution [J]. Chinese Journal of Catalysis, 2021, 42(7): 1137-1146.
https://doi.org/10.1016/S1872-2067(20)63728-7

[47] Wang Y, Yang W, Chen X, *et al*. Photocatalytic activity enhancement of core-shell structure g-C_3N_4@TiO_2 via controlled ultrathin g-C_3N_4 layer [J]. Applied Catalysis B: Environmental, 2018, 220: 337-347.
https://doi.org/10.1016/j.apcatb.2017.08.004

[48] Zhang W, Gu J, Lin J, *et al*. Photocatalytic degradation of jellyfish polyps: A sustainable approach to combat jellyfish blooms [J]. Marine Pollution Bulletin, 2025, 218: 118154.
https://doi.org/10.1016/j.marpolbul.2025.118154

[49] Wu S, Yan M, Zhong Y, *et al*. COF nanotubes/2D nanosheets heterojunction for superior photocatalytic bactericidal activity even at low concentration and weak light [J]. Journal of Hazardous Materials, 2025, 492: 138111.
https://doi.org/10.1016/j.jhazmat.2025.138111

[50] Ge C, Wang B, Yang H, *et al*. Direct Z-scheme GaSe/ZrS_2 heterojunction for overall water splitting [J]. International Journal of Hydrogen Energy, 2023, 48(36): 13460-13469.
https://doi.org/10.1016/j.ijhydene.2022.12.247

[51] Akbari M, Rasouli J, Rasouli K, *et al*. MXene-based composite photocatalysts for efficient degradation of antibiotics in wastewater [J]. Scientific reports, 2024, 14(1): 31498.
https://doi.org/10.1038/s41598-024-83333-3

[52] Yuan J, Wang B Y, Zong Y C, *et al*. Ce-MOF modified Ceria-based photocatalyst for enhancing the photocatalytic performance [J]. Inorganic Chemistry Communications, 2023, 153: 110799.
https://doi.org/10.1016/j.inoche.2023.110799

[53] Zhang H, Li M, Wang W, *et al*. Designing 3D porous BiOI/Ti_3C_2 nanocomposite as a superior coating photocatalyst for photodegradation of RhB and photoreduction of Cr(VI) [J]. Separation and Purification Technology, 2021, 272: 118911.
https://doi.org/10.1016/j.seppur.2021.118911

[54] Kan L, Mu W, Chang C, *et al*. Dual S-scheme graphitic carbon-doped α-Bi_2O_3/β-Bi_2O_3/Bi_5O_7 ternary heterojunction photocatalyst for the degradation of bisphenol A [J]. Separation and Purification Technology, 2023, 312: 123388. https://doi.org/10.1016/j.seppur.2023.12338

[55] Liu S, Chen J, Liu D, *et al*. Enhanced visible-light photocatalytic performance via in situ composition-transforming synthesis of $BiVO_4$/BiOBr photocatalyst [J]. Journal of Nanoparticle Research, 2019, 21(8): 191. https://doi.org/10.1007/s11051-019-4625-z